Clays and Clay Minerals, Vol. 49, No. 1, 81–91, 2001.

VERMICULITIZATION OF PHLOGOPITE IN METAGABBRO, CENTRAL TURKEY

FATMA TOKSOY-KÖKSAL, ASUMAN G. TÜRKMENOĞLU, AND M. CEMAL GÖNCÜOĞLU
Middle East Technical University, Department of Geological Engineering, 06531, Ankara, Turkey

Abstract—Dioctahedral vermiculite occurs in an isolated metagabbro klippe (Kurançalı Metagabbro) that belongs to the Central Anatolian Ophiolites from central Turkey. Both the metagabbro and the structurally underlying high-grade metamorphic rocks are intruded by granitic rocks. The Kurançalı Metagabbro is characterized by its well-developed compositional layering, and the presence of vermiculitized phlogopite-rich layers. Petrographic and mineralogic studies show that the primary mineral phases in the host rock are diopside, tschermakitic hornblende, Fe-rich phlogopite, and plagioclase. Secondary minerals are hornblende, actinolitic hornblende, Fe-rich phlogopite, and vermiculite. A two-phase history of alteration involving acidic weathering and alkaline metasomatism is suggested for the dioctahedral vermiculite and secondary Fe-rich phlogopite, respectively. The alteration of phlogopite to dioctahedral vermiculite proceeded both along cleavage planes and at crystal edges. The vermiculite is colorless to pale yellow with weak pleochroism and shows optical continuity with the parent mineral. Vermiculite flakes, analyzed semi-quantitatively by scanning electron microscope-energy dispersive analysis (SEM-EDS) and electron microprobe (EMP), are characterized by partially expanded interlayers, K depletion, and Mg and/or Al enrichment. X-ray diffraction (XRD) and differential thermal analysis-thermal gravimetric (DTA-TG) analyses indicate that phlogopite is not a pure phase, although it is the dominant one. The XRD patterns show the presence of both dioctahedral vermiculite having dehydrated interlayers and hydroxy-Al interlayers, and interstratified phlogopite-vermiculite. The transformation of phlogopite to vermiculite is thought to represent an initial stage of weathering in an acidic environment.

Key Words—Central Anatolian Ophiolites, Metagabbro, Mineral Weathering, Phlogopite, Vermiculite.

INTRODUCTION

Vermiculite is a mineral, resembling mica, which exfoliates by rapid heating. The name is for an expandable 2:1 phyllosilicate structure with a layer charge of $0.6 < x < 0.9$ per $O_{10}(OH)_2$ and with Mg, Fe^{3+} or hydroxy-Al complexes in the interlayer (Velde, 1985; de la Calle and Suquet, 1988; Moore and Reynolds, 1989). Numerous studies were performed on large vermiculite grains that were well characterized as trioctahedral vermiculite, according to the definition of Gruner (1934). Later studies reported vermiculite from soils that is either dioctahedral or trioctahedral (Hathaway, 1955; Barshad and Kishk, 1969; Douglas, 1989).

Most vermiculite forms by alteration of micas. The major elemental composition of vermiculites is closely related to that of the parent mica, although there is partial disruption of the mica structure (Jelitto *et al.*, 1993). Vermiculites resulting from the alteration of micas commonly involve the replacement of the interlayer K by a hydrated cation, generally Mg (Moore and Reynolds, 1989; Nemecz, 1981).

In soils, vermiculite is a common constituent and is unquestionably the product of low-temperature weathering. There is less certainty about the formation of macroscopic vermiculite which was attributed to either hydrothermal (Morel, 1955) and/or supergene processes (de la Calle and Suquet, 1988; Zhelyaskova-Panayotova *et al.*, 1992, 1993). According to experimental studies (Roy and Romo, 1957; Komarneni and Roy, 1981), vermiculite is a product of mica alteration by dilute low-alkali solutions.

A two-phase history of alteration was found in deposits in Turkey, that includes an earlier acidic weathering causing vermiculite and a later alkaline metasomatism resulting in secondary Fe-rich phlogopite formation. These processes were recognized in an ophiolitic metagabbro from Central Anatolian Ophiolites. In this paper, we report further on the formation of vermiculite resulting from phlogopite transformation process in this rock system.

GEOLOGY

The assemblage of magmatic and metamorphic rocks, known collectively as the Central Anatolian Crystalline Complex (CACC) (see "C" in Figure 1) consists of three main units: Central Anatolian Metamorphics (CAM), Central Anatolian Granitoids (CAG), and Central Anatolian Ophiolites (CAO). The metamorphic rocks present in the CACC are overthrusted by ophiolitic units, and both units are cut by granitoids (Göncüoğlu *et al.*, 1991, 1998; Göncüoğlu and Türeli, 1993; Yalınız *et al.*, 1996).

Unstratified and layered gabbroic rocks occurring as isolated outcrops in the CACC were shown to be parts of supra subduction in Late Cretaceous ophiolite (Yalınız *et al.*, 1996; Yalınız and Göncüoğlu, 1998). The gabbros have variable sizes and compositions ranging from fine grained to pegmatitic, and leuco- to

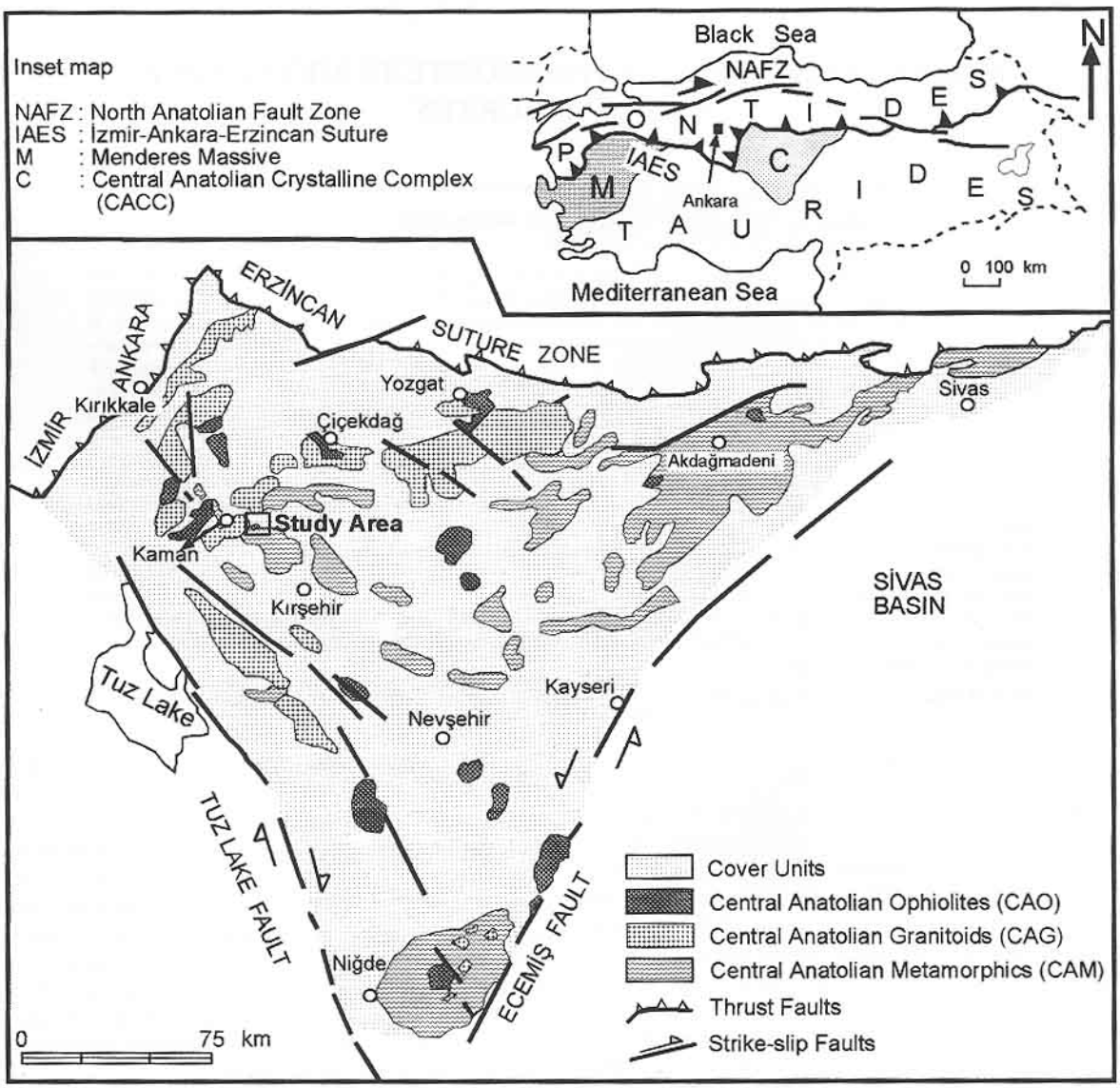

Figure 1. Simplified geological map of the Central Anatolian Crystalline Complex showing geological setting and main lithological units (after Yalınız and Göncüoğlu, 1998).

melano-gabbro, respectively. The studied layered metagabbros are located to the east of Kaman (Figure 1), and are characterized by dark mica (phlogopite). This outcrop, called Kurançalı Metagabbro, is observed within a tectonic sliver (Figure 2) having a sharp contact with the uppermost units of the CAM (Toksoy, 1998; Toksoy and Göncüoğlu, 1998; Toksoy-Köksal *et al.*, 2001). There is an intervening "sheared zone" between the allochthonous unit (Kurançalı Metagabbro) and the underlying metamorphics. All the units are cut by K-rich granitic dikes of the Kurançalı Granitoid belonging to CAG.

The Kurançalı Metagabbro, characterized by phlogopite, has clinopyroxene, hornblende, and plagioclase as primary minerals as well. The metagabbro is heterogeneous in composition and/or in particle size (from microscopic to pegmatitic) and shows modally graded rhythmic layering (Toksoy, 1998). Although compositional and petrographical variations vary widely as expressed by modal compositions of the mafic minerals, three main metagabbro types are identified in the field as clinopyroxene gabbro, hornblende gabbro, and phlogopite gabbro (Figure 2). The irregular-shaped bodies of the phlogopite-bearing gabbro consists mainly of phlogopite with lesser amounts of clinopyroxene. Phlogopite crystals are brittle, dark brown and black in color, and vary in size from 2 to 2.5 cm. Little plagioclase or hornblende is present in

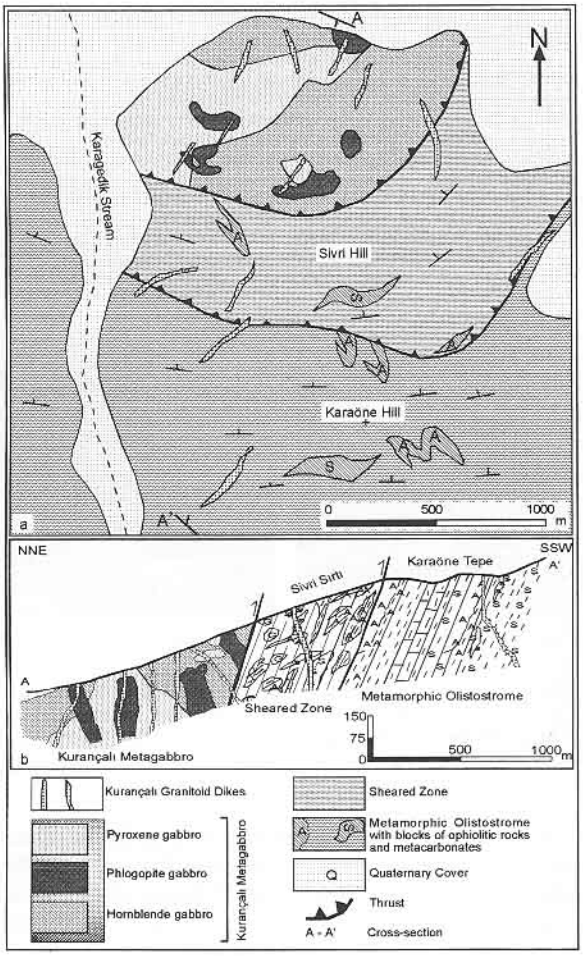

Figure 2. Geological map of the study area (after Toksoy-Köksal *et al.*, 2001).

the phlogopite gabbro. Most of the phlogopite gabbro outcrops are fresh but occasionally phlogopite shows signs of initial alteration to the gold-yellow color of vermiculite.

METHODS

Thin sections of 36 samples from the metagabbro were prepared following Kerr (1977) and examined optically by polarizing microscope. Four of these samples were mounted as chips on aluminum stubs and coated with gold. They were analyzed at 20 kV accelerating voltage from 80× to 5000× using a Jeol Ltd JSM-840A scanning electron microscope (SEM) equipped with a Tracor-Northern 5502 energy dispersive analysis system (EDS). The SEM-EDS study focused on the examination of crystal relationships and elemental changes semi-quantitatively.

Electron microprobe analyses were made on polished thin sections of four selected gabbro samples using a Jeol Superprobe 733 equipped with SEM and EDS. These samples were carbon coated and mounted on Al stubs using double stick tape. Elements Si, Al, Mg, and Na were analyzed using a proportional counter with a TAP (001) crystal of $2d$ = 25.757 Å, and Ca, Ti, and K were analyzed using a scintillation counter with a PET (002) crystal of $2d$ = 8.742 Å. In addition, Fe was analyzed using a scintillation counter with a LiF (002) crystal of $2d$ = 4.027 Å.

Using a Frantz isodynamic magnetic separator, ~100% pure phlogopite plus vermiculite fractions from eight gabbro samples were concentrated. Phlogopite could not be separated from vermiculitized portions because of the close association of phlogopite and vermiculite.

Powder X-ray diffraction (XRD) studies on the phlogopite and vermiculite samples were performed using a Rigaku Geiferflex X-ray diffractometer with Ni-filtered CuKα radiation at a voltage of 40 kV and current of 20 mV. Intensities were recorded on both oriented and random mounts at steps of 2 °2θ/min with a starting angle of 2 °2θ. Random samples, placed in a glass sample holder, were scanned to 70 °2θ whereas oriented samples on glass slides were scanned to either 30 or 40 °2θ. The d(060) values were measured only for untreated random mounts.

Ten oriented smear samples were prepared from a slurry with acetone and allowed to dry at room temperature to enhance basal reflections. Six oriented smear samples were heated at 170, 350, and 600°C for 1 h and also solvated with glycerol (G) and ethylene glycol (EG), separately (Jackson, 1975). Solvations with ethylene glycol and glycerol were performed on the oriented samples at 65°C for 24 h (vapor method) in a desiccator. Two of the remaining four smear samples were saturated by $MgCl_2$ and two were saturated by KCl for 13 h at room temperature following Jackson (1975). One each of the Mg-saturated smear samples was further solvated with 10% glycerol for 2 h at 60°C, and the K-saturated smear samples were further heated to 550°C. The heated, solvated, saturated, and air-dried samples were kept in a desiccator at 0% relative humidity until they were analyzed by XRD.

The thermal behavior of interstratified mica-vermiculite was investigated by differential thermal analysis (DTA) and thermal gravimetric (TG) analysis using a Rigaku DTA-TG apparatus. A Pt-$Pt_{90}Rh_{10}$ thermocouple was employed during the analyses. Samples weighing ~20 mg were analyzed by using calcined Al_2O_3 as a reference at static air atmosphere from room temperature to 1100°C, with a heating rate of 10°C/min.

Chemical analyses for three phlogopite separates of the vermiculite-bearing phlogopite gabbro were performed using an automated Perkin Elmer Optima 2000 standard inductively coupled plasma spectrometer (ICP). The same samples were decomposed in an orthophenanthroline complex to measure Fe^{2+} using a

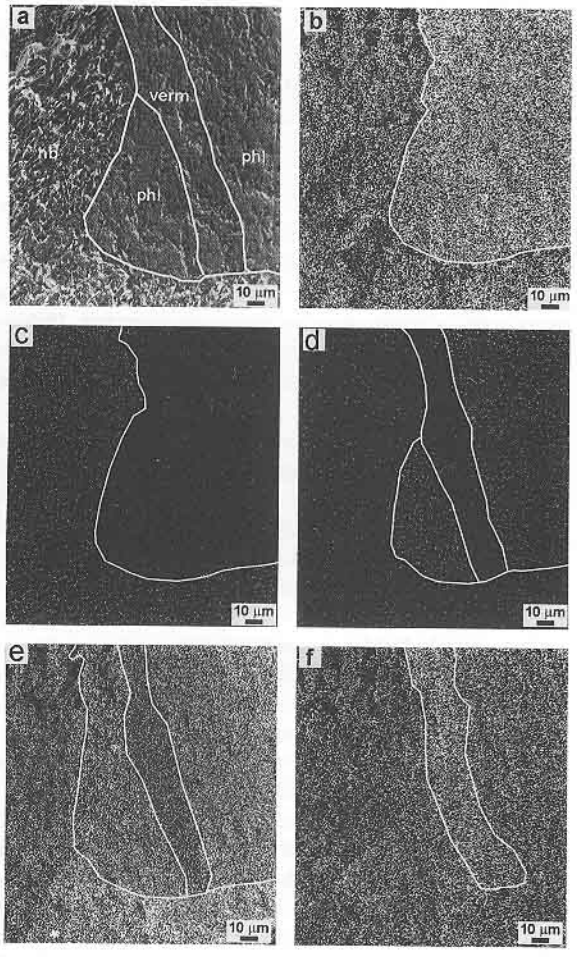

Figure 3. Electron microprobe photomicrographs showing elemental distributions and relationships among hornblende, phlogopite, and vermiculite. Photomicrographs: a) SEM image of the three phases, b) Al concentration, c) Ca concentration, d) K concentration, e) Si concentration, f) Mg concentration (hb: hornblende, phl: phlogopite, verm: vermiculite).

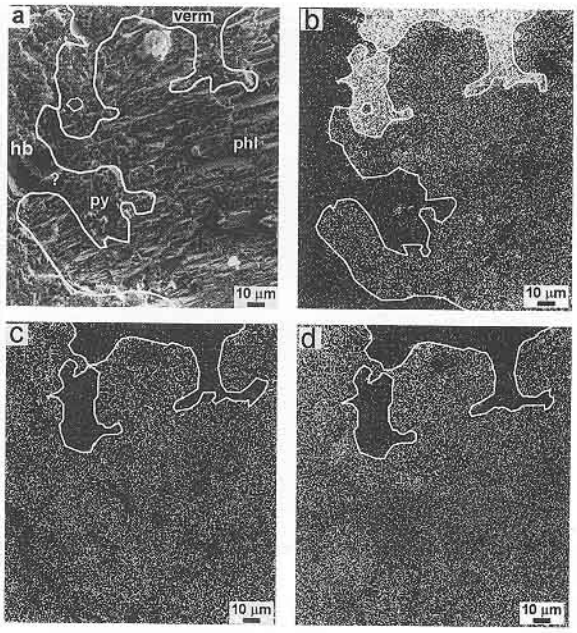

Figure 4. EMP photomicrographs showing elemental distributions and relationships among pyroxene, hornblende, phlogopite, and vermiculite. Photomicrographs: a) SEM image of the four phases, b) Al concentration, c) Mg concentration, d) Fe concentration (py: pyroxene, hb: hornblende, phl: phlogopite, verm: vermiculite).

Unicam SP 600 Series 2 spectrophotometer (Shapiro and Brannock, 1962). Using the chemical data, structural formulae of the phlogopite specimens were calculated in accordance with the method of Foster (1960), assuming the anhydrous form, on the basis of 22 oxygen atoms.

RESULTS

Semi-quantitative electron microprobe analysis

Boundary contacts between hornblende, phlogopite, and vermiculite phases were examined to determine elemental distributions because it was expected that Al and Ca would show opposing behavior (Figure 3a and 3b). Although the concentrations of these elements define the boundary between hornblende and phlogopite, phlogopite and vermiculite are not differentiated. In a single phlogopite crystal the narrow zones of low K and Si but high Mg concentration (Figure 3c–3e) show the presence of vermiculite, because K is replaced by Mg whereas Si is replaced by Al during the transformation of phlogopite to vermiculite (Deer *et al.*, 1980).

The concentration of Al is variable (Figure 4a) in a sample containing clinopyroxene, hornblende, phlogopite, and vermiculite. The highest concentration of Al is inversely related to Mg and Fe (Figure 4b and 4c). The zone with the highest Al, the lower K, and the lowest Mg and Fe concentrations (Figure 4d) represents Al-rich vermiculite. The zone showing medium Al and K concentration is phlogopite. The zone with the lowest Al concentration, higher Mg and Ca concentrations and slightly higher Fe concentration is probably hornblende. The zone with the lowest Al, and lower Fe probably is clinopyroxene.

Scanning electron microscope-energy dispersive X-ray analysis

Clinopyroxene is a primary phase in all samples studied whereas micas are either primary or secondary (Toksoy and Öner, 1997). Primary phlogopite booklets are large and easily identifiable by SEM and secondary phlogopite flakes are fine grained and form thin books at edges and cleavage surfaces of clinopyroxene and hornblende crystals. Vermiculite with platy morphology is associated with primary phlogopite and is partially expanded (Figure 5a and 5b). EDS analyses indicated semi-quantitatively the presence of higher

Ca compared to K within vermiculite flakes (Figure 5c). EDS spectra along a profile across phlogopite flakes with altered parts to vermiculite show a close association in composition and morphology of vermiculite and phlogopite and may imply a transformation (Barnhisel and Bertsch, 1989).

Petrographic study

The metagabbro samples are composed primarily of clinopyroxene, phlogopite, hornblende, and plagioclase in varying amounts. The secondary minerals are hornblende (uralite) replacing clinopyroxene; actinolitic hornblende replacing primary hornblende; Fe-rich phlogopite replacing clinopyroxene and secondary hornblende; vermiculite replacing phlogopitic mica; calcite, "sericite", and albite replacing plagioclase; and rarely epidote in clinopyroxene and plagioclase. The accessory minerals are sphene, magnetite, and hematite.

Fe-rich phlogopite is the essential mineral of the phlogopite gabbro, although it is also present in variable amounts in the other gabbro types. The primary phlogopite is characterized by strong brown pleochroism and it is in large plates, some of which have ragged terminations. The yellowish to reddish-brown colored phlogopite shows bright interference colors of second and third order and the optic axial angle (2V) is 2–8°. It shows parallel extinction and usually occurs together with diopsidic augite, magnetite, and sphene.

Alteration of phlogopite to vermiculite is poorly developed along cleavages and at rims (Figure 6). Relics of phlogopite, parallel to the cleavage planes, are common in altered crystals. Both altered and relic modes of occurrence, together with the textural features described above, indicate that this brown phlogopite is primary. Oxidation during the transformation of phlogopite to vermiculite caused high relief and numerous iron oxide inclusions along fractures and cleavage planes (Figure 6). Meunier and Velde (1979) and Rowins *et al.* (1991) indicated that in initial stages of weathering, alteration of phlogopite to vermiculite is limited but there is a strong tendency for iron to migrate to grain edges where it accumulates as iron oxides.

Vermiculite forming at the expense of phlogopite plates displays optical continuity with the parent mineral. Vermiculite is colorless to pale yellow with very weak pleochroism, and shows parallel extinction and very weak interference color.

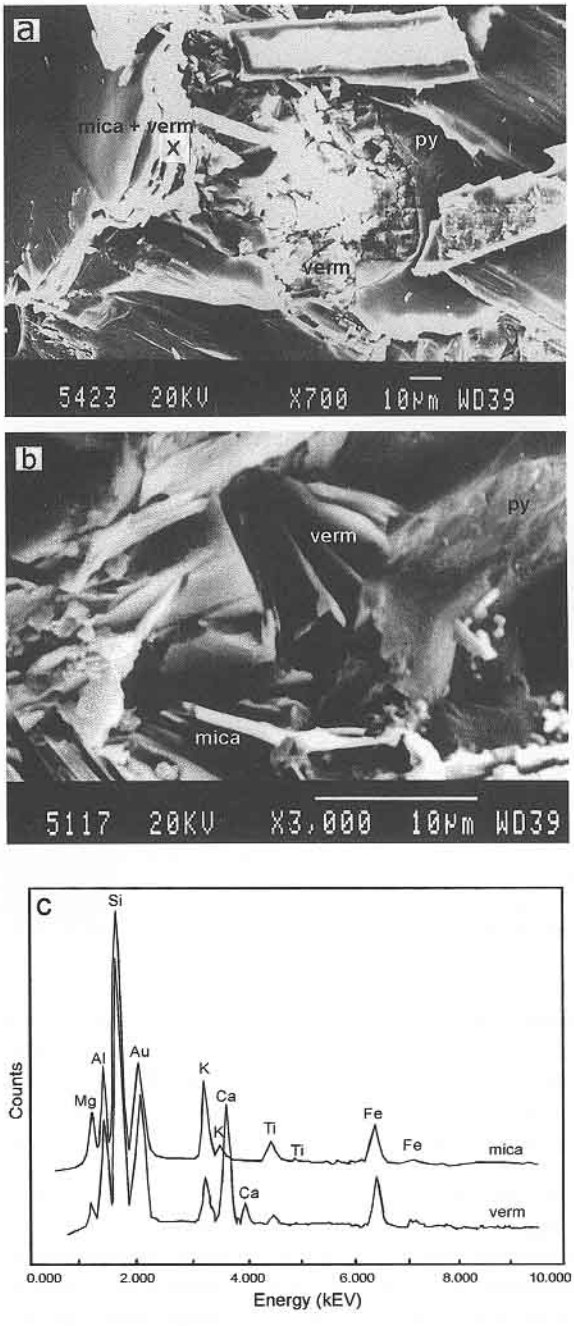

Figure 5. SEM photomicrographs showing expansible vermiculite crystals a) within mica crystals, b) together with dark mica and pyroxene crystals, and c) EDS spectra of vermiculite and mica taken from X area in photograph (a) (verm: vermiculite, mica: primary phlogopite or secondary Fe-rich phlogopite, py: pyroxene).

X-ray diffraction analysis

XRD patterns of all of the analyzed phlogopite are similar. Oriented specimens have strong first-order basal spacings of 10.1 Å and a rational series of peaks at 5.11, 3.38, and 2.52 Å (Figure 7). The (060) reflection of random samples is 1.541 Å, which indicates a trioctahedral mica according to Chen (1977) and Bailey (1980) (Figure 8). The XRD data (Table 1; Figures 7 and 8) and the chemical data are consistent with phlogopite-2M_1.

XRD analysis showed that the phlogopite contains vermiculite (see Douglas, 1989), because there are

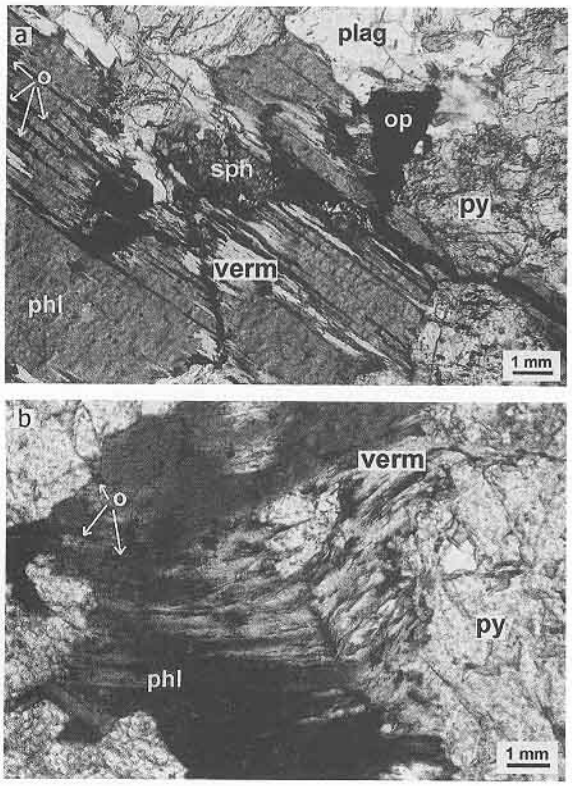

Figure 6. Photomicrographs showing vermiculitized phlogopite crystals a) along cleavage surfaces together with a high amount of opaques and b) along cleavage surfaces and at rims (phl: phlogopite, verm: vermiculite, py: pyroxene, plag: plagioclase, sph: sphene, op: opaque, o: tiny oxide inclusions due to oxidation).

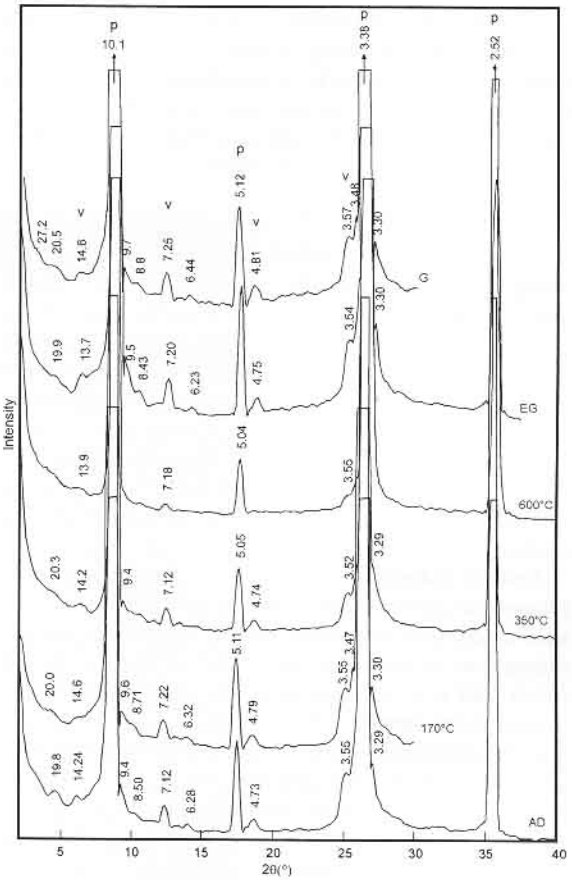

Figure 7. X-ray diffraction patterns of an oriented sample of vermiculitized phlogopite representing all the analyzed samples (AD: air-dried, EG: ethylene glycol, G: glycerol, heating to 170, 350, and 600°C; p: phlogopite, v: vermiculite).

small, broad peaks with basal spacings of 13.7–14.6, 7.12–7.25, 4.73–4.81, and 3.47–3.57 Å, and low-intensity reflections near 9.4, 6.28, and 3.29 Å (Figure 7). However, intensities and shapes of the vermiculite peaks (Figure 7) are not typical of data from the literature and may reflect the small amount of vermiculite. The (060) reflection of vermiculite is 1.506 Å (Figure 8) which indicates a dioctahedral vermiculite (Douglas, 1989). These data suggest the presence of dioctahedral vermiculite of two types, a two-layer hydrate with a 14-Å spacing and a dehydrated type with a 9.4-Å spacing.

The 9.4-Å and 3.29-Å reflections of dehydrated vermiculite and the 3.55-Å reflection of two-layer hydrate vermiculite cause peak asymmetry of the phlogopite reflections. Asymmetric tailing of the X-ray reflections on the low angle side is tentatively identified as related to a mixture of two of more layer silicates (Meunier and Velde, 1979). This asymmetry is observed as separate peaks where the alteration degree of phlogopite and, thus, the proportion of vermiculite is higher. The interstratification is not obvious on the (001) reflection but it is easily observed near the 3.38-Å peak of the

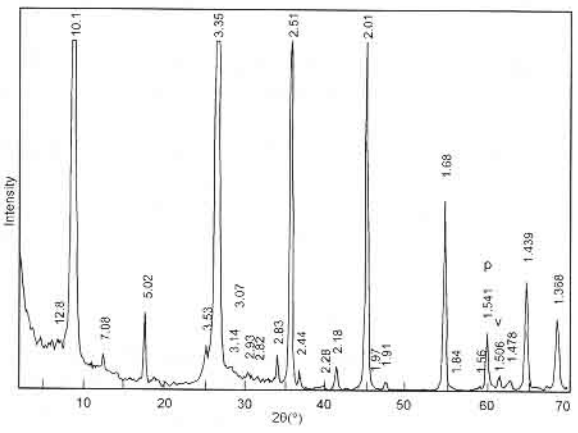

Figure 8. X-ray diffraction patterns of a random sample of vermiculitized phlogopite representing all the analyzed samples (p: phlogopite, v: vermiculite).

Table 1. XRD data for $2M_1$ phlogopite from literature and for the analyzed mica samples from the phlogopite Kurançalı Metagabbro.

	Data from the literature				Data of the analyzed samples from the Kurançali Metagabbro			
	1		2		FT-25		FT-51	
hkl	*d*(Å)	I	*d*(Å)	I	*d*(Å)	I	*d*(Å)	I
002	10.12	10	10.125	vs	10.18	vs	10.13	vs
004	5.06	2	5.034	w	5.08	w	5.057	w
11$\bar{4}$	3.54	4	3.540	w	3.53	w	3.54	w
006	3.36	10	3.361	m	3.39	m	3.37	m
11$\bar{4}$	3.283	4	3.282	w	—	—	—	—
11$\bar{5}$	3.16	1	3.155	vw	3.14	vw	3.16	vw
025	3.04	4	3.038	m	3.07	m	—	—
11$\bar{5}$	2.93	1	2.923	vw	2.93	vw	2.94	vw
11$\bar{6}$	2.818	2	2.817	w	2.82	w	—	—
116	2.624	8	2.624	vs	2.63	vs	2.62	vs
008	2.522	4	2.519	vw	2.52	s	2.52	s
13$\bar{3}$	—	—	2.437	m	2.44	m	2.44	m
13$\bar{5}$	—	—	2.272	vw	2.28	vw	2.29	vw
135	—	—	2.181	m	2.18	m	2.18	m
060	—	—	1.538	m	1.541	m	1.541	m

Note: 1. $2M_1$ phlogopite (Chen, 1977). 2. $2M_1$ phlogopite (Bailey, 1984). I (intensity): vs = very strong; w = weak; m = medium; vw = very weak.

phlogopite (Figure 7). In addition to these asymmetries, there is also a weak 19.8-Å basal reflection suggesting random interstratification of 10.1-Å phlogopite and 9.4-Å dehydrated vermiculite.

The analyzed samples were separately saturated with ethylene glycol and glycerol to determine expansion behavior and type of the vermiculite. The XRD patterns of the vermiculites and the interstratification of phlogopite and vermiculite show no expansion after saturation with either ethylene glycol or glycerol. This behavior also indicates the presence of dehydrated vermiculite (Douglas, 1989).

The contraction behavior of the two-hydrate vermiculite and dehydrated vermiculite was also examined by heating at 170, 350, and 600°C (Figure 7). Peak intensities at 3.55 and 3.29 Å, which occur as shoulders of the 3.39-Å reflection of phlogopite, become less intense with increasing temperature. Similarly, the 9.4-Å reflection of dehydrated vermiculite persists as a shoulder of the 10.1-Å reflection of phlogopite.

Smear mounts of the samples that were Mg-saturated (air-dried) and Mg-saturated with glycerol show expansion with the 13.2-Å (002) vermiculite peak increasing to 14.2 Å with an increase in intensity (Figure 9). The K-saturated air-dried sample does not show a change of the 13.2-Å peak, but heating of the K-saturated sample at 550°C involves contraction. This behavior of vermiculite suggests the presence of a hydroxy-Al interlayer (Douglas, 1989). Dehydrated vermiculite is not evident on XRD patterns of Mg- and K-saturated samples.

Negligible expansion as indicated by the basal spacings at 9.4 and 14 Å with ethylene glycol and glycerol, incomplete contraction on heating, expansion and/or an increase in intensity of basal spacings of (002) and (004) by glycerol solvation following Mg-saturation, and contraction on heating at 550°C following K-saturation in these samples are consistent with the hydroxy-Al interlayer in the two-layer hydrate and dehydrated types of vermiculite (April and Newton, 1983; Buurman *et al.*, 1988; Barnhisel and Bertsch, 1989; Douglas, 1989; Argast, 1991).

Thermal analysis

DTA analyses show broad and shallow endothermic reactions occurring over a wide range of temperatures from ~300 to ~750–800°C (Figure 10). This slight endothermic reaction is interpreted to be related to very slow dehydroxlylation of the vermiculitized parts of the phlogopite. The broad and very shallow endothermic effect between 300–600°C is thought to represent the gradual release of strongly held interlayer water in the vermiculitized material (Zhelyaskova-Panayotova *et al.*, 1992). These specimens also show a small and broad exothermic peak at ~900°C, which is a characteristic feature of vermiculite and probably represents the recrystallization of new oxide phases. Note that as the slope of the dehydration curve between 300 and 750–800°C becomes less steep (note dash lines, Figure 10) the height of the exothermic curve becomes smaller. This observation may indicate that such samples have a lower amount of the altered component, vermiculite. The very slow dehydration rate is accompanied by small inflections in the TG-curve (Figure 11). Two samples (FT-43 and FT-51) show continuous weight loss from ~10 to 1100°C whereas others display stepwise weight losses varying

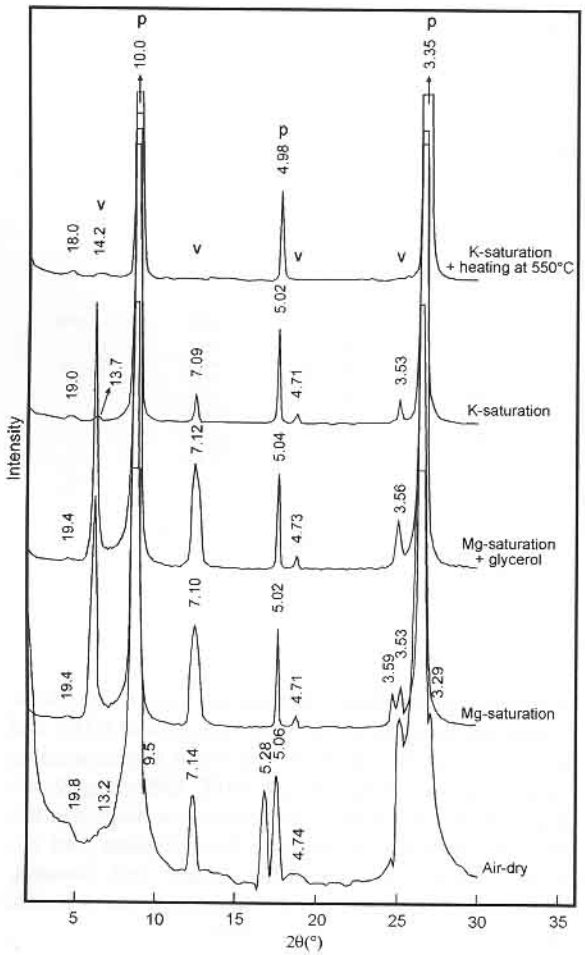

Figure 9. X-ray diffraction patterns of an oriented sample of vermiculitized phlogopite representing all the analyzed samples after saturation with $MgCl_2$ and KCl, and subsequent treatments (p: phlogopite, v: vermiculite).

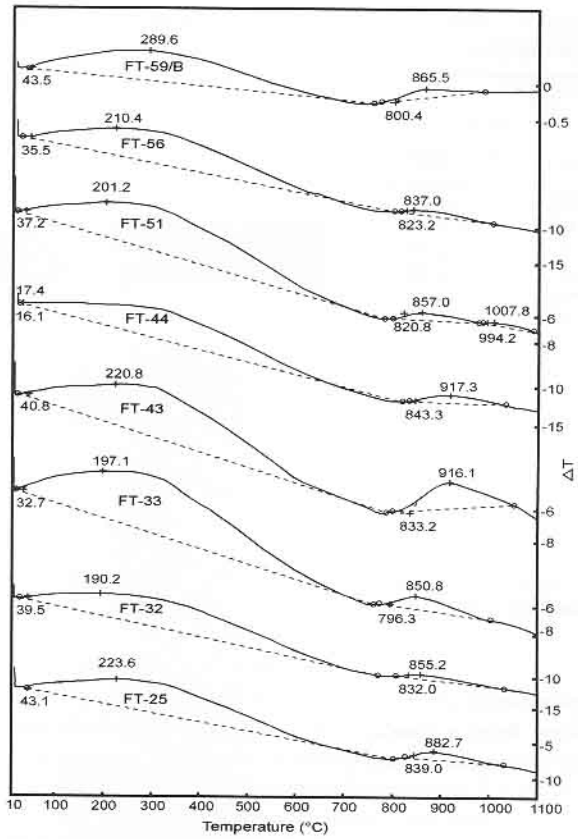

Figure 10. DTA curves of the studied vermiculitized phlogopite samples (FT-25 to FT-59/B: sample numbers).

from 0.7 to 2.5%. Phlogopite produces a curve without a pronounced deflection (Grim, 1968) upon heating to 1000°C.

The simultaneous DTA-TG measurements from the Kurançalı Metagabbro samples support the presence of phlogopite with varying amounts of vermiculite or interstratified phlogopite-vermiculite phases.

Inductively coupled plasma spectrometry analysis

Results of the ICP analysis are expressed in oxide form (wt. %) and the compositions of representative phlogopites are given in Table 2. Reddish-brown, purplish-greenish dark mica is classified following Reider *et al.* (1988) as phlogopite, as $phlogopite_{(57-70)}$-$annite_{(30-43)}$. These data are in good agreement with the results of petrographic, XRD, and thermal analyses.

DISCUSSION

The early Upper Cretaceous Kurançalı Metagabbro consists of varying amounts of clinopyroxene, primary and secondary amphibole, primary and secondary dark micas (phlogopite and Fe-rich phlogopite, respectively), and plagioclase. It is primarily characterized by the presence of phlogopite and its alteration product, vermiculite. The phlogopite is of primary origin whereas the secondary Fe-rich phlogopite is the alteration product of clinopyroxene and amphibole reacting with K-rich solutions from intruding Late Cretaceous granitic dikes.

The most characteristic feature of the phlogopite metagabbro is the transformation of phlogopite to vermiculite. Vermiculite is intercalated with hydroxy-cation complexes (not developed into complete sheets) rather than hydrated cations in the interlayer, because the vermiculite does not collapse on heating or expand on glycerol or ethylene-glycol saturation, but it does expand by Mg-saturation with glycerol solvation and contract by K-saturation with heating at 550°C. Based on the XRD data, two forms of dioctahedral vermiculite were identified, a hydroxy-Al and dehydrated vermiculite in accordance with Douglas (1989).

The occurrence of interstratified phlogopite-vermiculite observed here is similar to those that are generally accepted to form during transformation of mica to vermiculite (*e.g.,* Fanning *et al.,* 1989). In this case,

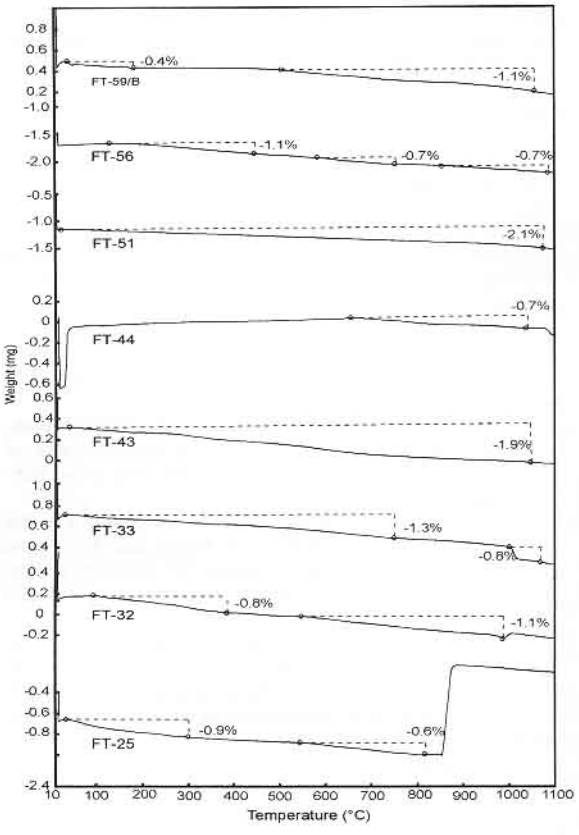

Figure 11. TG curves of the studied vermiculitized phlogopite samples (FT-25 to FT-59/B: samples numbers).

Table 2. Results of ICP analyses for dark micas from the phlogopite Kurançali Metagabbro, Central Anatolia, Turkey.

	Samples		
	FT-32	FT-43	FT-59/B
SiO_2	41.11	39.10	38.35
Al_2O_3	13.89	15.89	15.86
TiO_2	2.81	2.63	2.86
FeO	11.23	13.67	10.62
Fe_2O_3	5.9	6.02	5.92
MgO	12.50	10.34	13.82
CaO	0.23	0.44	0.20
Na_2O	0.25	0.22	0.27
K_2O	8.91	8.39	8.77
[1]LOI	2.65	2.67	2.80
Total	99.48	99.37	99.47
Si	5.955	5.826	5.693
^{IV}Al	2.045	2.174	2.307
^{VI}Al	0.327	0.206	0.433
Ti	0.306	0.506	0.315
Fe^{2+}	0.644	0.653	0.653
Fe^{3+}	1.361	1.662	1.302
Mg	2.698	2.239	3.019
Ca	0.036	0.069	0.032
Na	0.070	0.063	0.078
K	1.647	1.556	1.640
[2]Fe : Mg	0.3352	0.4260	0.3013
[3]f_{com}	64.82	71.32	54.48

[1] Loss on ignition.
[2] $Fe : Mg = Fe^{2+}/(Fe^{2+} + Mg^{2+})$.
[3] $f_{com} = [(2Fe_2O_3 + FeO) \times (2Fe_2O_3 + FeO + MgO)^{-1}] \times 100$.

the transformation of phlogopite to vermiculite requires a structural change from trioctahedral to dioctahedral hydroxy-Al and dehydrated forms as indicated by chemical changes.

The most commonly observed transformation of phlogopite to vermiculite involves the loss of interlayer K and the introduction of a hydrated Mg-Fe-Al interlayer (Banfield and Eggleton, 1988; Moon *et al.*, 1994). This mechanism proceeds by releasing K, Si, and Ti, and requires the addition of small amounts of Mg, Fe, or Al besides H_2O and O_2, and the oxidation of ferrous to ferric iron. Oxidation is compensated by the redistribution of octahedral Al (replacing Si in the tetrahedral sheet) and the loss of octahedral cations. The loss of octahedral cations in phlogopite during weathering in an acidic environment may result in the replacement by Al. This process favors the development of hydroxy-Al interlayers in the vermiculite near the crystal surface (May *et al.*, 1979; Douglas, 1989; Moon *et al.*, 1994) to form the aluminous dioctahedral vermiculite. According to Moon *et al.* (1994), the initial stage of transformation of phlogopite to vermiculite proceeds by a continuous decrease of Al-for-Si tetrahedral substitutions and a progressive increase of Al-for-(Mg–Fe^{2+}) octahedral substitutions with weathering. The excess Al is assumed to be involved in the interlayer occupancy.

The elemental changes from phlogopite to vermiculite (K-depletion, slight decrease in Si, Al-enrichment) were observed by semi-quantitative electron microprobe analyses although these changes were not detected by wet chemical analyses because of the limited amount of vermiculite present.

In this study, additional Al required for the formation of the hydroxy-Al variety of dioctahedral vermiculite is assumed to be derived from the weathering and alteration of plagioclase in the metagabbro. Vicente *et al.* (1977), Holdren and Berner (1979), and Argast (1991) also suggested that Al for hydroxy-Al interlayers can be precipitated from an aqueous species derived from the simultaneous weathering and dissolution of associated feldspar as well as its derivation from the phlogopite.

The origin of the trioctahedral variety of vermiculite remains unclear (Justo *et al.*, 1986; de la Calle and Suquet, 1988; Zhelyaskova-Panayotova *et al.*, 1992, 1993) whereas the dioctahedral variety is unquestionably accepted as the product of low-temperature surface weathering (Gruner, 1939; Hathaway, 1955; Barshad and Kishk, 1969; April *et al.*, 1986; Graham *et al.*, 1989; Moon *et al.*, 1994). Experimental studies produced vermiculite as an alteration product of micas

owing to the effects of low-alkali solutions (Komarneni and Roy, 1981).

Two geochemical events are recorded in the mineralogical assemblage of the studied metagabbro. They are (1) an early weathering event in a low pH environment and (2) a later alkaline event which coincided with a nearby intrusion of granitic dikes. Early in this study, the assumption was made that there is a continuous alteration sequence of clinopyroxene → secondary hornblende → secondary Fe-rich phlogopite → vermiculite because all dark micas were assumed to represent secondary Fe-rich phlogopite. However, further study showed that phlogopite is the primary magmatic phase as well as clinopyroxene and hornblende. Thus, both primary magmatic phlogopite and secondary Fe-rich phlogopite are present in the studied metagabbro samples. The formation of the green-brown Fe-rich phlogopite (in clinopyroxene, hornblende, and phlogopite) is interpreted to result from K-metasomatism, related to the intrusion of K-rich granitic dikes of the CAG. Vermiculite from secondary Fe-rich phlogopite was not recognized by optical microscopy. In contrast, the formation of vermiculite is found to be a reaction which only involves the primary phlogopite.

These high-alkali content solutions related to the granitic dike intrusions can not be responsible for the occurrence of vermiculite from phlogopite. The amount of vermiculite is low and it is only related to phlogopite. Therefore, K-rich solutions probably limited the formation of vermiculite from phlogopite and prevented its formation from Fe-rich phlogopite. Previous studies (Vali and Hesse, 1992) and petrographical-mineralogical data obtained in this study indicate that the dioctahedral hydroxy-Al and dehydrated vermiculite from primary trioctahedral phlogopite unquestionably represent an initial stage of weathering in an acidic environment.

ACKNOWLEDGMENTS

This paper is a part of an M.Sc. study of the first author at the Department of Geological Engineering in Middle East Technical University. The authors thank the Scientific and Technical Research Council of Turkey (BAYG-TÜBİTAK) for the research scholarship given to the first author. The authors thank W.D. Huff for the review of the manuscript and his kind suggestions and corrections. The authors also gratefully acknowledge the valuable suggestions and editing of S. Guggenheim, W.C. Elliott, and A. Mermut and for the significant improvement of the manuscript.

REFERENCES

April, R.H. and Newton, R.M. (1983) Mineralogy and chemistry of some Adirondack Spodosols. *Soil Science*, **135,** 301–307.

April, R.H., Hluchy, M.M., and Newton, R.M. (1986) The nature of vermiculite in Adirondack soils and till. *Clays and Clay Minerals*, **34,** 549–556.

Argast, S. (1991) Chlorite vermiculitization and pyroxene etching in an aeolian periglacial sand dune, Allen County, Indiana. *Clays and Clay Minerals*, **39,** 622–633.

Bailey, S.W. (1980) Structures of layer silicates. In *Crystal Structures of Clay Minerals and Their X-Ray Identification*, G.W. Brindley and G. Brown, eds., Mineralogical Society, London, 1–123.

Bailey, S.W. (1984) Review of cation ordering in micas. *Clays and Clay Minerals*, **32,** 81–92.

Banfield, J.F. and Eggleton, R.A. (1988) Transmission electron microscope study of biotite weathering. *Clays and Clay Minerals*, **36,** 382–403.

Barnhisel, R.I. and Bertsch, P.M. (1989) Chlorites and hydroxy-interlayered vermiculite and smectite. In *Minerals in Soil Environments. 2nd edition.* J.B. Dixon and S.B. Weed, eds., Soil Science Society of America, Madison, Wisconsin, 729–788.

Barshad, I. and Kishk, F.M. (1969) Chemical composition of soil vermiculite as related to their genesis. *Contribution to Mineralogy and Petrology*, **24,** 136–155.

Buurman, P., Meijer, E.L., and van Wijck, J.H. (1988) Weathering of chlorite and vermiculite in ultramafic rocks of Cabo Ortegal, Northwestern Spain. *Clays and Clay Minerals*, **36,** 263–269.

Chen, P.-Y. (1977) *Table of Key Lines in the X-Ray Powder Diffraction Patterns of Minerals in Clays and Associated Rocks.* Department of Natural Resources, Geological Survey Occasional Paper 21, Authority of the State of Indiana, Bloomington, Indiana, 67 pp.

de la Calle, C. and Suquet, H. (1988) Vermiculite. In *Hydrous Phyllosilicates (Exclusive of Micas)*, S.W. Bailey, ed., Mineralogical Society of America, Washington, D.C., 455–496.

Deer, W.A., Howie, R.A., and Zussman, J. (1980) *An Introduction to Rock Forming Minerals, 12th edition.* Longman, London, 528 pp.

Douglas, L.A. (1989) Vermiculites. In *Minerals in Soil Environments, 2nd edition*, J.B. Dixon and S.B. Weed, eds., Soil Science Society of America, Madison, Wisconsin, 635–668.

Fanning, D.S., Keramidas, V.Z., and El-Desoky, M.A. (1989) Micas. In *Minerals in Soil Environments, 2nd edition*, J.B. Dixon and S.B. Weed, eds., Soil Science Society of America, Madison, Wisconsin, 522–624.

Foster, M.D. (1960) *Interpretation of the Composition of Trioctahedral Micas.* U.S. Geological Survey Professional Paper 354-B, Washington, D.C., 11–49.

Göncüoğlu, M.C. and Türeli, K. (1993) Petrology and geodynamic interpretation of plagiogranites from Central Anatolian ophiolites (Aksaray-Türkiye). *Doğa - Türk Yerbilimleri Dergisi*, **2,** 195–203.

Göncüoğlu, M.C., Toprak, G.M.V., Kuşçu, I., Erler, A., and Olgun, E. (1991) *Orta Anadolu Masifinin Batı Bölümünün Jeolojisi Bölüm II: Güney Kesim.* Turkish Petroleum Corporation Report 2909, 140 pp. (in Turkish).

Göncüoğlu, M.C., Yalınız, M.K., Özgül, L., and Toksoy, F. (1998) *Orta Anadolu Ofiyolitlerinin Petrojenezi: Izmir-Ankara-Erzincan Okyanus Kolunun Evrimine bir Yaklaşım.* Scientific and Technical Research Council of Turkey Report, 61 pp. (in Turkish).

Graham, R.C., Weed, S.B., Bowen, L.H., Amarasiriwardena, D.D., and Buol, S.W. (1989) Weathering of iron-bearing minerals in soils and saprolite on the North Carolina Blue Ridge Front: II. Clay mineralogy. *Clays and Clay Minerals*, **37,** 29–40.

Grim, R.E. (1968) *Clay Mineralogy, 2nd edition.* McGraw-Hill, New York, 596 pp.

Gruner, J.W. (1934) Structures of vermiculites and their collapse by dehydration. *American Mineralogist*, **19,** 557–575.

Gruner, J.W. (1939) Ammonium mica synthesized from vermiculite. *American Mineralogist*, **24,** 428–435.

Hathaway, J.C. (1955) Studies of some vermiculite type clay minerals. *Clays and Clays Minerals*, 74–86.

Holdren, G.R., Jr. and Berner, R.A. (1979) Mechanisms of feldspar weathering—I. Experimental studies. *Geochimica et Cosmochimica Acta,* **43,** 1161–1171.

Jackson, M.L. (1975) *Soil Chemical Analysis—Advanced Course, 2nd edition.* Published by the author, Madison Wisconsin, 53705, 895 pp.

Jelitto, J., Dubinska, E., Wiewiora, A., and Bylina, P. (1993) Layer silicates from serpentinite-pegmatite contact (Wiry, Lower Silesia, Poland). *Clays and Clay Minerals,* **41,** 693–701.

Justo, A., Maqueda, C., and Perez Rodriguez, J.L. (1986) Estudio quimico de vermiculitas de Andalicia y Badajoz. *Boletin de la Sociedad Espafiola de Mineral,* **9,** 123–129.

Kerr, P.F. (1977) *Optical Mineralogy, 4th edition.* McGraw-Hill Book Company, New York, 492 pp.

Komarneni, S. and Roy, R. (1981) Hydrothermal transformations in candidate overpack materials and their effects on Cesium and strontium sorption. *Nuclear Technology,* **54,** 118–122.

May, H., Helmke, P., and Jackson, M. (1979) Gibbiste solubility and thermodynamic properties of hyroxy-aluminum ions in aqueous solution at 25°C. *Geochimica et Cosmochimica Acta,* **43,** 861–868.

Meunier, A. and Velde, B. (1979) Biotite weathering in granites of Western France. In *Developments in Sedimentology,* M.M. Mortland and V.C. Farmer, eds., Elsevier Scientific Publishing Company, New York, 405–412.

Moon, H.S., Song, Y., and Lee, S.Y. (1994) Supergene vermiculitization of phlogopite and biotite in ultramafic and mafic rocks, Central Korea. *Clays and Clay Minerals,* **42,** 259–268.

Moore, D.M. and Reynolds, R.C., Jr. (1989) *X-ray Diffraction and the Identification and Analysis of Clay Minerals.* Oxford University Press, Oxford, 332 pp.

Morel, S.W. (1955) Biotite in the basement complex of Southern Nyasaland. *Geological Magazine,* **92,** 241–255.

Nemecz, E. (1981) *Clay Minerals.* Akademiai Kiado, Budapest, Hungary, 547 pp.

Rieder, M., Cavazzini, G., D'yakonov, Y.S., Frank-Kamenetskii, V.A., Gottardi, G., Guggenheim, S., Koval, P.V., Müller, G., Nieva, M.R., Radoslovich, E.W., Robert, J.-L., Sassi, F.P., Takeda, H., Weiss, Z., and Wones, D.R. (1998) Nomenclature of the micas. *Clays and Clay Minerals,* **46,** 586–595.

Rowins, S.M., Lalonde, A.E., and Cameron, E.M. (1991) Magmatic oxidation in the syenitic Murdock Creek intrusion, Kirkland Lake, Ontario: Evidence from the ferromagnesian silicates. *Geological Journal,* **99,** 395–414.

Roy, R. and Romo, L.A. (1957) Weathering studies: I New data on vermiculite. *Geology Journal,* **65,** 603–610.

Shapiro, L. and Brannock, W.W. (1962) *Rapid Analysis of Silicate, Carbonate and Phosphate Rock.* U.S. Geological Survey Bulletin 1144-A, Washington, D.C., 1–56.

Toksoy, F. (1998) Petrography and mineralogy of the vermiculitised phlogopitic metagabbro from the Kurançalı area (Kırşehir-Central Anatolia). M.S. thesis, Middle East Technical University, Ankara, Turkey, 175 pp.

Toksoy, F. and Göncüoğlu, M.C. (1998) Phlogopitic metagabbro within Central Anatolian Ophiolites, Kurançalı (Kırşehir), Turkey. *3rd International Turkish Geology Symposium, Middle East Technical University, 31 August–4 September, 1998, Ankara-Turkey, Abstracts,* 175.

Toksoy, F. and Öner, A. (1997) Vermicultization process. *13th National Electron Microscopy Congress with International Participation, Middle East Technical University, September 1–4, 1997, Ankara-Turkey, Proceedings,* 761–768.

Toksoy-Köksal, F., Göncüoğlu, M.C., and Yalınız, K. (2001) Petrology of the Kurancalı phlogopitic metagabbro: An island arc-type ophiolitic sliver in the Central Anatolian Crystalline Complex, Turkey. *International Geological Review,* (in press).

Vali, H. and Hesse, R. (1992) Identification of vermiculite by transmission electron microscopy and x-ray diffraction. *Clay Minerals,* **27,** 185–192.

Velde, B. (1985) *Clay Minerals (Physico-Chemical Explanation of their Occurences). Developments in Sedimentology Volume 40.* Elseiver, Amsterdam, 427 pp.

Vicente, M.A., Razzaghe, M., and Robert, M. (1977) Formation of aluminum hydroxy vermiculite (intergrade) and smectite from mica under acidic conditions. *Clay Minerals,* **12,** 101–112.

Yalınız, M.K. and Göncüoğlu, M.C. (1998) General geological characteristics and distribution of the Central Anatolian Ophiolites. *Hacettepe Üniversitesi Yerbilimleri Dergisi,* **20,** 19–30.

Yalınız, M.K., Floyd, P.A., and Göncüoğlu, M.C. (1996) Supra-subduction zone ophiolites of Central Anatolia: Geochemical evidence from the Sarıkaraman Ophiolite, Aksaray, Turkey. *Mineralogical Magazine,* **60,** 697–710.

Zhelyaskova-Panayotova, M., Laskou, M., Economou, M., and Stefanov, D. (1992) Vermiculite occurrences from the Vavdos and Gerakini Areas of the W. Chalkidiki Peninsula, Greece. *Chemical Erde,* **52,** 41–48.

Zhelyaskova-Panayotova, M., Economou-Eliopoulos, M., Petrov, P.M., Laskou, M., and Alexandrova, A. (1993) Vermiculite deposits in the Balkan Peninsula. *Bulletin of Geological Society of Greece,* **28,** 451–461.

E-mail of corresponding author: ftkoksal@metu.edu.tr; ftkoksal@geologist.com

(Received 23 February 2000; accepted 8 September 2000; Ms. 430; A.E. W. Crawford Elliott)